

Square-root topological phase with time-reversal and particle-hole symmetry

Tsuneya Yoshida,¹ Tomonari Mizoguchi,¹ Yoshihito Kuno,¹ and Yasuhiro Hatsugai¹

¹*Department of Physics, University of Tsukuba, Ibaraki 305-8571, Japan*

(Dated: March 25, 2021)

Square-root topological phases have been discussed mainly for systems with chiral symmetry. In this paper, we analyze the topology of the squared Hamiltonian for systems preserving the time-reversal and particle-hole symmetry. Our analysis elucidates that two-dimensional systems of class CII host helical edge states due to the nontrivial topology of the squared Hamiltonian in contrast to the absence of ordinary topological phases. The emergence of the helical edge modes is demonstrated by analyzing a toy model. We also show the emergence of surface states induced by the non-trivial topology of the squared Hamiltonian in three dimensions.

I. INTRODUCTION

In these decades, topological aspects of condensed matter systems are extensively studied^{1,2}. A typical example of topological insulators is an integer quantum Hall system³⁻⁵ where the non-trivial topology in the bulk induces chiral edge modes, i.e., bulk-edge correspondence⁶. The topology in the bulk is enriched for systems preserving Altland-Zirnbauer (AZ) symmetry^{7,8}, i.e., the time-reversal symmetry^{9,10}, particle-hole symmetry¹¹, and chiral symmetry¹². These variety of topological phases are systematically understood by the ten-fold way classification¹³⁻¹⁶; the classification result predicts the presence/absence of topological phases for a given d -dimensional system in an AZ symmetry class. After this progress, topological insulators/superconductors have been extended to various systems; for instance, in these years, higher-order topological insulators¹⁷⁻²⁰ and non-Hermitian topological insulators²¹⁻²³ are actively studied.

Among these extensions, Arkininstall *et al.*²⁴ proposed square-root topological insulators, which provides a novel insight to topological phases. They have analyzed a one-dimensional tight-binding model and have demonstrated that the system hosts edge modes induced by the topology of the squared Hamiltonian rather than the original Hamiltonian. After this proposal, analysis of square-root topological insulators in higher dimensions has been addressed²⁵⁻³², which has elucidated ubiquity of the square-root topological phases. For instance, a square-root counterpart of higher-order topological phases are reported by both theoretical²⁵ and experimental works^{33,34}. In addition, Refs. 25 and 27 suggested that for chiral symmetric systems (class AIII) a toy model can be systematically constructed by decorating a lattice³⁵.

Despite of the above progress, square-root topology has not sufficiently explored for systems preserving time-reversal symmetry and particle-hole symmetry³⁶.

In this paper, we analyze systems with time-reversal symmetry and particle-hole symmetry in terms of the square-root perspective. Our analysis elucidates that non-trivial topology of the squared Hamiltonian predicts helical edge modes in two-dimensional systems in class CII [i.e., the systems preserving time-reversal symmetry

and the particle-hole symmetry, see Eq. (1a)-(1c)] in contrast to the absence of ordinary two-dimensional topological phases in this class. We also propose a method to construct toy models of square-root topological phases which is a complementary to the method employed in the previous works²⁵⁻²⁷. Applying our approach to systems of class CII, we demonstrate the emergence of surface Dirac cones for a three-dimensional system as well as the emergence of helical edge modes in a two-dimensional systems.

In Sec. II, we elucidates that the helical edge modes emerge due to the non-trivial topology of the squared Hamiltonian. Applying our approach to construct toy models [see Sec. III], we analyze square-root topological phases for other cases of dimensions and symmetry classes in Sec. IV. A short summary is given in Sec. V. Appendices are devoted to the topological invariants of the squared Hamiltonian and technical details.

II. SQUARE-ROOT PERSPECTIVE ON TWO-DIMENSIONAL SYSTEMS OF CLASS CII

We show that square-root topology of two-dimensional systems in class CII induces helical edge modes [see Fig. 1], in contrast to the absence of the ordinary two-dimensional topological phases in this class³⁷.

A. Symmetry constraints on the squared Hamiltonian

Consider a two-dimensional Hamiltonian $H(\mathbf{k})$ in class CII [see Eq. (1a)-(1c)]. We show that topology of the squared Hamiltonian $H_{\text{sq}}(\mathbf{k}) := H^2(\mathbf{k})$ can be characterized by a \mathbb{Z}_2 -invariant of two-dimensional systems in class AII.

Let us consider a Hamiltonian $H(\mathbf{k})$ which preserves time-reversal, particle-hole and chiral symmetry

$$TH(\mathbf{k})T^{-1} = H(-\mathbf{k}), \quad (1a)$$

$$CH(\mathbf{k})C^{-1} = -H(-\mathbf{k}), \quad (1b)$$

$$\Gamma H(\mathbf{k})\Gamma^{-1} = -H(\mathbf{k}), \quad (1c)$$

with $\mathbf{k} := (k_x, k_y)$ denoting the momentum. Here, T and C are anti-unitary operators satisfying $[T, C] = 0$. The unitary operator Γ satisfies $\Gamma^2 = 1$. For symmetry class CII, relations $T^2 = C^2 = -1$ and $\Gamma = TC$ are satisfied.

The above symmetry constraints result in the following relations

$$TH_{\text{sq}}(\mathbf{k})T^{-1} = H_{\text{sq}}(-\mathbf{k}), \quad (2a)$$

$$CH_{\text{sq}}(\mathbf{k})C^{-1} = H_{\text{sq}}(-\mathbf{k}), \quad (2b)$$

$$\Gamma H_{\text{sq}}(\mathbf{k})\Gamma^{-1} = H_{\text{sq}}(\mathbf{k}), \quad (2c)$$

with $H_{\text{sq}}(\mathbf{k}) := H^2(\mathbf{k})$.

Equation (2c) and the relation $\Gamma^2 = 1$ indicate that $H_{\text{sq}}(\mathbf{k})$ can be block-diagonalized in the plus and minus sectors of Γ . The Hamiltonian of the plus [minus] sector $H_{\text{sq},+}(\mathbf{k})$ [$H_{\text{sq},-}(\mathbf{k})$] satisfies

$$TH_{\text{sq},+(-)}(\mathbf{k})T^{-1} = H_{\text{sq},+(-)}(\mathbf{k}). \quad (3)$$

In addition, in the plus (minus) sector, the operator C is written as $C = -T$ ($C = T$) due to the relations $\Gamma = TC$ and $T^2 = -1$.

Therefore, $H_{\text{sq},\pm}$ effectively preserves the time-reversal symmetry; $TH_{\text{sq},\pm}(\mathbf{k})T^{-1} = H_{\text{sq},\pm}(-\mathbf{k})$ with $T^2 = -1$ which results in quantization of the \mathbb{Z}_2 -invariant in class AII (see Sec. II B).

B. Equivalence of the \mathbb{Z}_2 -invariants of the plus and minus sectors

In the previous section, we have seen that the squared Hamiltonian in each subsector $H_{\text{sq},\pm}$ preserves the time-reversal symmetry with $T^2 = -1$. Therefore, the topology of $H_{\text{sq},\pm}$ can be characterized by the \mathbb{Z}_2 -invariant $\nu = 0, 1 \pmod{2}$. In this section, we show that $H_{\text{sq},+}(\mathbf{k})$ and $H_{\text{sq},-}(\mathbf{k})$ have the same topology.

1. Brief review of the \mathbb{Z}_2 -invariant

Let us start with the definition of \mathbb{Z}_2 -invariants ν_{\pm} . For square-lattice systems, ν_{\pm} are defined as^{9,38}

$$\nu_{\pm} = \frac{1}{2\pi i} \left[\int_{-\pi}^{\pi} dk_x [A_{\pm,x}(k_x, \pi) - A_{\pm,x}(k_x, 0)] - \int_{-\pi}^{\pi} dk_x \int_{-\pi}^0 dk_y F_{\pm}(\mathbf{k}) \right], \quad (4)$$

with $-\pi \leq k_{\mu} < \pi$ ($\mu = x, y$). We note that the integral in the last term is taken over a half of the Brillouin zone (BZ). The Berry connection $A_{\pm,\mu}(\mathbf{k})$ and the Berry curvature $F(\mathbf{k})$ are defined as

$$A_{\pm,\mu}(\mathbf{k}) = \sum_{ns} \langle u_{\pm n}^s(\mathbf{k}) | \partial_{\mu} u_{\pm n}^s(\mathbf{k}) \rangle, \quad (5a)$$

$$F_{\pm}(\mathbf{k}) = \partial_x A_{\pm,y}(\mathbf{k}) - \partial_y A_{\pm,x}(\mathbf{k}), \quad (5b)$$

with ∂_{μ} denoting derivative with respect to k_{μ} . Here, $|u_{\pm n}^s(\mathbf{k})\rangle$ denote the eigenstates of $H_{\text{sq},\pm}(\mathbf{k})$ with $n =$

$1, 2, \dots$ and $s = \text{I, II}$ which label the energy bands³⁹. At the time-reversal invariant momenta, eigenstates specified by (n, I) and (n, II) form a Kramers pair.

We note that for computation of the \mathbb{Z}_2 -invariant [Eq. (4)], the following gauge should be taken.

$$|u_{\pm n}^{\text{I}}(-\mathbf{k})\rangle = T|u_{\pm n}^{\text{II}}(\mathbf{k})\rangle, \quad (6a)$$

$$|u_{\pm n}^{\text{II}}(-\mathbf{k})\rangle = -T|u_{\pm n}^{\text{I}}(\mathbf{k})\rangle. \quad (6b)$$

As we see below,

$$\nu_+ = \nu_- \pmod{2}, \quad (7)$$

holds, meaning that $H_{\text{sq},+}(\mathbf{k})$ and $H_{\text{sq},-}(\mathbf{k})$ has the same topology.

2. Proof of Eq. (7)

We show that $H_{\text{sq},+}(\mathbf{k})$ and $H_{\text{sq},-}(\mathbf{k})$ have the same topology.

Firstly, we note a relation between $|u_{+n}^s(\mathbf{k})\rangle$ and $|u_{-n}^s(\mathbf{k})\rangle$. Consider the case where the energy eigenvalues are non-zero and the Hamiltonian $H(\mathbf{k})$ is written as⁴⁰

$$H(\mathbf{k}) = \begin{pmatrix} 0 & Q(\mathbf{k}) \\ Q^{\dagger}(\mathbf{k}) & 0 \end{pmatrix}, \quad (8)$$

with $N \times N$ -matrix $Q(\mathbf{k})$ which maps a state in the minus sector of Γ to a state in the plus sector. In this basis, the time-reversal operator can be written as

$$T = \begin{pmatrix} U_T & 0 \\ 0 & U_T \end{pmatrix} \mathcal{K}, \quad (9)$$

where U_T is the unitary matrix⁴¹ satisfying $U_T^T = -U_T$, and \mathcal{K} is the operator of complex conjugation.

In this case, the normalized eigenvectors $|u_{-n}^s(\mathbf{k})\rangle$ can be written as

$$|u_{-n}^s(\mathbf{k})\rangle = \frac{1}{\sqrt{\epsilon_{\text{sq},+sn}(\mathbf{k})}} Q^{\dagger}(\mathbf{k}) |u_{+n}^s(\mathbf{k})\rangle, \quad (10)$$

with the normalized eigenvectors $|u_{+n}^s(\mathbf{k})\rangle$. Here, eigenvalues of $H(\mathbf{k})$ are assumed to be non-zero (i.e., eigenvalues $\epsilon_{\text{sq},+sn}(\mathbf{k})$ of the squared Hamiltonian $H_{\text{sq},+}$ are positive). In addition, $|u_{-n}^s(\mathbf{k})\rangle$ satisfy the time-reversal constraint [Eq. (6)], provided that $|u_{+n}^s(\mathbf{k})\rangle$ satisfy it.

Now, we prove Eq. (7). Firstly, we note

$$A_{-, \mu}(\mathbf{k}) = A_{+, \mu}(\mathbf{k}) + f_{\mu}(\mathbf{k}), \quad (11a)$$

with

$$f_{\mu}(\mathbf{k}) = \frac{1}{\sqrt{\epsilon_{\text{sq},+sn}(\mathbf{k})}} \text{tr} [P_+(\mathbf{k}) Q(\mathbf{k}) \left(\partial_{\mu} \frac{1}{\sqrt{\epsilon_{\text{sq},+sn}(\mathbf{k})}} Q^{\dagger}(\mathbf{k}) \right)], \quad (11b)$$

$$P_+(\mathbf{k}) = \sum_{ns} |u_{+n}^s(\mathbf{k})\rangle \langle u_{+n}^s(\mathbf{k})|. \quad (11c)$$

Here, the summation is taken over ‘‘occupied states’’. (Here, we define ‘‘occupied states’’ as follows: setting an energy to specify the gap, we can regard the ‘‘occupied states’’ as eigenstates whose energy is smaller than it.)

By applying Stokes’ theorem we can see that the integrals of f_μ vanishes because $f_\mu(\mathbf{k})$ is gauge independent. Therefore, we can see that Eq. (7) holds.

C. Analysis of a toy model

Following an approach described in Sec. III we construct a toy model of the square-root topological phase of class CII in two dimensions. Our analysis demonstrates the presence of helical edge states induced by the square-root topology.

1. Energy spectrum and topological characterization

Suppose that the operators of time-reversal symmetry, particle-hole symmetry, and chiral symmetry are written as

$$T = s_2\tau_3\rho_0\mathcal{K}, \quad (12a)$$

$$C = s_1\tau_2\rho_0\mathcal{K}, \quad (12b)$$

$$\Gamma = s_3\tau_1\rho_0, \quad (12c)$$

where s ’s, τ ’s, and ρ ’s are the Pauli matrices.

Here, we show that the following two-dimensional Hamiltonian possesses the square-root topology:

$$H(\mathbf{k}) = H_D(\mathbf{k}) + mU, \quad (13a)$$

$$H_D(\mathbf{k}) = p_1(\mathbf{k})s_1\tau_0\rho_0 + p_2(\mathbf{k})s_3\tau_2\rho_2 + p_3(\mathbf{k})s_3\tau_3\rho_2, \quad (13b)$$

with $\mathbf{k} = (k_x, k_y)$ denoting the momentum and $U = s_1\tau_1\rho_0$. Prefactors are defined as $p_1(\mathbf{k}) = 2t \sin k_x$, $p_2(\mathbf{k}) = 2t \sin k_y$, and $p_3(\mathbf{k}) = 2t(\cos k_x + \cos k_y) - \mu$ with real numbers t and μ .

Noting the commutation relation, $[H_D(\mathbf{k}), U] = 0$, we can compute $H_{\text{sq}}(\mathbf{k}) = H^2(\mathbf{k})$ as

$$H_{\text{sq}}(\mathbf{k}) = [p^2(\mathbf{k}) + m^2]s_0\tau_0\rho_0 + 2m[p_1(\mathbf{k})s_0\tau_1\rho_0 + p_2(\mathbf{k})s_2\tau_3\rho_2 - p_3(\mathbf{k})s_2\tau_2\rho_2], \quad (14)$$

with $p^2(\mathbf{k}) = p_1^2(\mathbf{k}) + p_2^2(\mathbf{k}) + p_3^2(\mathbf{k})$.

The above Hamiltonian $H_{\text{sq}}(\mathbf{k})$ can be block-diagonalized with $\Gamma = s_3\tau_1\rho_0$. The plus sector is spanned by

$$|+a\rangle = \frac{1}{\sqrt{2}} \begin{pmatrix} 1 \\ 0 \end{pmatrix}_s \begin{pmatrix} 1 \\ 1 \end{pmatrix}_\tau \begin{pmatrix} 1 \\ 0 \end{pmatrix}_\rho, \quad (15a)$$

$$|+b\rangle = \frac{1}{\sqrt{2}} \begin{pmatrix} 0 \\ 1 \end{pmatrix}_s \begin{pmatrix} 1 \\ -1 \end{pmatrix}_\tau \begin{pmatrix} 1 \\ 0 \end{pmatrix}_\rho, \quad (15b)$$

$$|+c\rangle = \frac{1}{\sqrt{2}} \begin{pmatrix} 1 \\ 0 \end{pmatrix}_s \begin{pmatrix} 1 \\ 1 \end{pmatrix}_\tau \begin{pmatrix} 0 \\ 1 \end{pmatrix}_\rho, \quad (15c)$$

$$|+d\rangle = \frac{1}{\sqrt{2}} \begin{pmatrix} 0 \\ 1 \end{pmatrix}_s \begin{pmatrix} 1 \\ -1 \end{pmatrix}_\tau \begin{pmatrix} 0 \\ 1 \end{pmatrix}_\rho. \quad (15d)$$

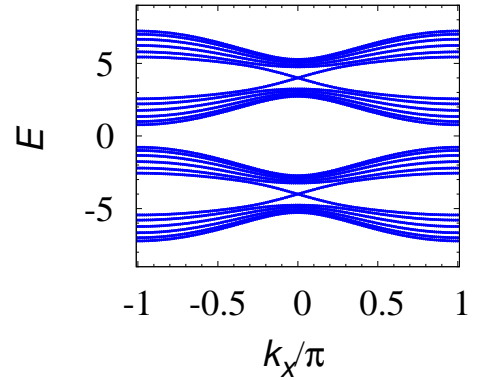


FIG. 1. Energy spectrum for $t = 0.5$, $\mu = 1.3$, and $m = 4$. These data are obtained by imposing the periodic (open) boundary condition along the x - (y -) direction. Along the y -direction $L_y = 6$ sites are aligned.

In this subsector, the Hamiltonian is written as

$$H_{\text{sq},+}(\mathbf{k}) = 2m[p_1(\mathbf{k})\chi_3\rho_0 + p_2(\mathbf{k})\chi_2\rho_2 + p_3(\mathbf{k})\chi_1\rho_2], \quad (16)$$

where we have omitted the term proportional to the identity matrix [i.e., the first term of Eq. (14)]. Matrices χ ’s are the Pauli matrices. The above result is obtained by straight forward calculations, e.g.,

$$s_2\tau_3\rho_2\Psi_+ = \Psi_+ \begin{pmatrix} & -1 \\ & 1 \\ 1 & \\ -1 & \end{pmatrix} := \Psi_+\chi_2\sigma_2, \quad (17)$$

with

$$\Psi_+ = (|+a\rangle |+b\rangle |+c\rangle |+d\rangle). \quad (18)$$

Because $H_{\text{sq},+}(\mathbf{k})$ preserves the time-reversal symmetry with $T = \chi_2\sigma_0\mathcal{K}$ ($T^2 = -1$, $T = -C$)⁴², the topological properties can be characterized by the \mathbb{Z}_2 -invariant [see Eq. (4)]. In the presence of the inversion symmetry, the \mathbb{Z}_2 -invariant ν_+ can be computed from the parity of ‘‘occupied states’’ at the time-reversal invariant momenta⁴³. Noting that $H_{\text{sq},+}(\mathbf{k})$ satisfies $PH_{\text{sq},+}(\mathbf{k})P^{-1} = H_{\text{sq},+}(-\mathbf{k})$ with $P = \chi_1\rho_2$, we can see that among the time-reversal invariant momenta $(0,0)$, $(\pi,0)$, $(0,\pi)$, and (π,π) , the parity eigenvalue of the ‘‘occupied band’’ is plus only at $(0,0)$. Because the product of the parity eigenvalues at the time-reversal invariant momenta is minus⁴⁴, we have $\nu_+ = 1$.

The square-root topology of the Hamiltonian (13a) characterized by $\nu_+ = 1$ predicts edge modes. In Fig. 1, we plot the band structure obtained under the cylinder geometry [i.e., the periodic (open) boundary condition is imposed along the x - (y -) direction]. In this figure, we can find the helical edge modes around $E \sim \pm 4$.

The above results elucidate that for two-dimensional systems of class CII, helical edge modes emerge due to non-trivial topology of the squared Hamiltonian despite the ordinary two-dimensional topological phases are absent in this class.

III. APPROACH TO CONSTRUCT TOY MODELS

We describe our approach to construct a toy model of a square-root topological phase which is complementary to the method employed in previous works^{25–27}. Our approach is available when the following two conditions are satisfied. (i) There exists a topological phase described by a Hamiltonian which preserves an additional symmetry [see Eq. (19)]. (ii) The presence/absence of the additional symmetry does not affect the topology of the squared Hamiltonian.

A. Generic framework

When the presence/absence of the additional symmetry does not affect the topology of the squared Hamiltonian, a Hamiltonian with the additional symmetry serves a toy model. This is because topology of the squared Hamiltonian is equivalent to the topology of the original Hamiltonian.

In the following, we show that topology of the squared Hamiltonian is equivalent to the topology of the original Hamiltonian in the presence of the additional symmetry. Consider a Hamiltonian in a given symmetry class (e.g., class CII) whose squared Hamiltonian with additional symmetry is topologically nontrivial. Here, the additional symmetry is described by the commutation relation of the squared Hamiltonian and a unitary matrix U [$U^2 = \mathbb{1}$] which also preserves the AZ symmetry; for instance in the case of class CII, U satisfies

$$TUT^{-1} = U, \quad (19a)$$

$$CUC^{-1} = -U, \quad (19b)$$

$$\Gamma U \Gamma^{-1} = -U. \quad (19c)$$

By making use of the adiabatic continuation, we can deform the squared Hamiltonian to

$$H'_{\text{sq}}(\mathbf{k}) = \sum_{i=1, \dots, d+1} p_i(\mathbf{k}) \tilde{\gamma}_i, \quad (20)$$

where $\tilde{\gamma}$'s are Hermitian matrix satisfying $\{\tilde{\gamma}_i, \tilde{\gamma}_j\} = 2\delta_{ij}$ for $i, j = 1, \dots, d+1$ and $[\tilde{\gamma}_i, U] = 0$ for $i = 1, \dots, d+1$. Here, $p(\mathbf{k})$'s are scalars which are chosen so that $H'_{\text{sq}}(\mathbf{k})$ is reduced to the gapped Dirac Hamiltonian [for instance see, just below of Eq. (13a)].

Thanks to the additional symmetry, we can find the square-root Hamiltonian $H(\mathbf{k})$ of the above simplified model. Namely, the square-root Hamiltonian, which preserves the symmetry constraints, is written as

$$H(\mathbf{k}) = H_{\text{D}}(\mathbf{k}) + mU, \quad (21a)$$

$$H_{\text{D}}(\mathbf{k}) = \sum_{i=1, \dots, d+1} p_i(\mathbf{k}) \gamma_i, \quad (21b)$$

where the matrices $\gamma_i = U \tilde{\gamma}_i$ satisfy $\{\gamma_i, \gamma_j\} = 2\delta_{ij}$ for $i, j = 1, \dots, d+1$. This fact can be seen by a straightfor-

ward calculation:

$$H^2(\mathbf{k}) = (p^2(\mathbf{k}) + m^2)\mathbb{1} + 2mUH_{\text{D}}(\mathbf{k}), \quad (22)$$

with $p^2(\mathbf{k}) = \sum_{i=1, \dots, d+1} p_i^2(\mathbf{k})$ and $\mathbb{1}$ being the identity matrix. The above result indicates that in the presence of the additional symmetry [see Eq. (19)], the topology of the squared Hamiltonian is identical to the topology of the original Hamiltonian.

Therefore, we can construct the toy model in a given symmetry class by obtaining $H_{\text{D}}(\mathbf{k})$ in the following steps. (i) Define the operators of the given symmetry class. (ii) Introduce U satisfying Eq. (19). (iii) Prepare the gapped Dirac Hamiltonian $H_{\text{D}}(\mathbf{k})$ so that $H_{\text{D}}(\mathbf{k})$ preserves the additional symmetry as well as the AZ symmetry.

B. A remark on topology of two-dimensional systems in class CII

We note that for class CII, the presence of the additional symmetry does not change the topological properties. As we have seen in Sec. IIA, the topology of the squared Hamiltonian is described by $H_{\text{sq},+}$ and $H_{\text{sq},-}$ which preserve time-reversal symmetry. Equation (19) indicates that no further constraint is imposed on $H_{\text{sq},\pm}$. The additional symmetry just requires that the topology of $H_{\text{sq},+}$ and that of $H_{\text{sq},-}$ are the same, which is satisfied even without the additional symmetry (see Sec. IIB 2). Therefore, our approach can be applied to construct a two-dimensional model of class CII [see Sec. IIC 1].

IV. APPLICATION TO OTHER SYMMETRY CLASSES

As we have seen in Sec. IIIA, a toy model of a given symmetry class can be constructed by considering the system with the additional symmetry when the additional symmetry does not change the topology. In other words, a necessary condition for our approach to be applicable is that for a given symmetry class and dimensions, there exists a topological phase in a system with the additional symmetry⁴⁵.

In Sec. IVA, we elucidate when a topological phase exists in the presence of the additional symmetry by addressing the corresponding topological classification. The obtained classification results help us to find a toy model showing square-root topology in two dimensions for class AIII [see Sec. IVB], and in three dimensions in class CII [see Sec. IV C].

A. Topological classifications of systems with the additional symmetry

The topological classification for systems with the additional symmetry can be carried out by analyzing the

symmetry of the block-diagonalized Hamiltonian with the unitary matrix U ($U^2 = 1$). Classification results of topological phases with the additional symmetry are summarized in Table I.

class of $H(\mathbf{k})$	T	C	Γ	$d = 1$	$d = 2$	$d = 3$
A	0	0	0	0	\mathbb{Z}	0
AIII	0	0	1	0	\mathbb{Z}	0
AI	1	0	0	0	0	0
BDI	1	1	1	0	0	0
D	0	1	0	0	\mathbb{Z}	0
DIII	-1	1	1	0	\mathbb{Z}_2	\mathbb{Z}_2
AII	-1	0	0	0	\mathbb{Z}_2	\mathbb{Z}_2
CII	-1	-1	1	0	\mathbb{Z}_2	\mathbb{Z}_2
C	0	-1	0	0	\mathbb{Z}	0
CI	1	-1	1	0	0	0

TABLE I. Classification results of d -dimensional topological insulators/superconductors with the additional symmetry [see Eqs. (1a)-(1c)]. The second, the third, and the fourth columns specify a type of the corresponding operators; ± 1 in the second [the third] column represents the sign of $T^2 = \pm 1$ [$C^2 = \pm 1$]. (“0” denotes that the corresponding symmetry is absent.) We note that the absence of chiral symmetry or particle-hole symmetry allows U to be the identity matrix. Thus, topological insulators in class A, AI, AII are ordinary topological insulators.

As explained in Appendix B, the classification results are the same for each of the following three groups: (i) symmetry classes A, AIII, D, and C; (ii) symmetry classes AI, BDI, and CI; (iii) symmetry classes AII, DIII, and CII. This is because the particle-hole symmetry and chiral symmetry are not closed in the subsector of U .

Table I indicates that in the presence of the additional symmetry, there exists a topological phase for a two-dimensional system in class AIII and for a three-dimensional system in class CII.

By making use of these results, we demonstrate the presence of the square-root topological phases whose topology is maintained even in the absence of the additional symmetry.

B. Two-dimensional system in class AIII

Consider a Hamiltonian $H(\mathbf{k})$ for a two-dimensional system with chiral symmetry [see Eq. (1c)]. As mentioned in Sec. II A, the squared Hamiltonian $H_{\text{sq}}(\mathbf{k})$ can be block-diagonalized with subsectors of the chiral operator Γ ($\Gamma^2 = 1$).

The squared Hamiltonian $H_{\text{sq},\pm}(\mathbf{k})$ of the plus (minus) sector preserves no symmetry and its topology is characterized by the Chern number [see Eq. (C1)]. As explained in Appendix C, the Chern number for the plus sector should be equal to the Chern number for the minus

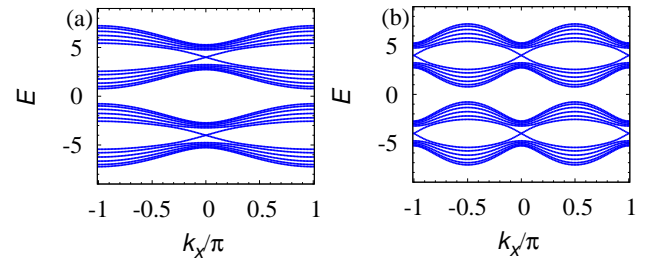


FIG. 2. Energy spectrum obtained under the cylinder geometry. Panel (a) is obtained for $p_1(\mathbf{k}) = 2t \sin k_x$, $p_2(\mathbf{k}) = 2t \sin k_y$, and $p_3(\mathbf{k}) = 2t(\cos k_x + \cos k_y) - \mu$. Panel (b) is obtained for $p_1(\mathbf{k}) = 2t \sin 2k_x$, $p_2(\mathbf{k}) = 2t \sin k_y$, and $p_3(\mathbf{k}) = 2t(\cos 2k_x + \cos k_y) - \mu$. In this case, the Chern number takes two $N_{\text{Ch},+} = 2$ inducing two chiral edge modes. These data are obtained for $t = 0.5$, $\mu = 1.3$, and $m = 4$.

sector. In addition, the presence/absence the additional symmetry does not affect the topology (see Appendix C).

Therefore, our approach is available for two-dimensional systems in class AIII. In the following, we see that a toy model indeed hosts a chiral edge state induced by the square-root topology.

1. Edge modes and the topological characterization

Let us consider a Hamiltonian of 4×4 -matrix. The operator of chiral symmetry is given by

$$\Gamma = s_0 \tau_3. \quad (23)$$

The operator U satisfying Eq. (19c) can be chosen as $U = \sigma_0 \tau_1$.

In this case, we can construct the following Hamiltonian preserving the symmetry

$$H(\mathbf{k}) = H_{\text{D}}(\mathbf{k}) + m \sigma_0 \tau_1, \quad (24a)$$

$$H_{\text{D}}(\mathbf{k}) = p_1(\mathbf{k}) \sigma_1 \tau_1 + p_2(\mathbf{k}) \sigma_2 \tau_1 + p_3(\mathbf{k}) \sigma_3 \tau_1, \quad (24b)$$

where $\mathbf{k} = (k_x, k_y)$ denotes the momentum. Prefactors p_i ($i = 1, 2, 3$) are defined just below Eq. (13a).

The squared Hamiltonian can be block-diagonalized with the matrix $\Gamma = s_0 \tau_3$. The Hamiltonian in the plus sector is written as

$$H_{\text{sq},+}(\mathbf{k}) = [p^2(\mathbf{k}) + m^2] \sigma_0 + 2m[p_1(\mathbf{k}) \sigma_1 + p_2(\mathbf{k}) \sigma_2 + p_3(\mathbf{k}) \sigma_3]. \quad (25)$$

We can see that the Chern number $N_{\text{Ch},+}$ [for the definition see Eq. (C1)] takes one, predicting the presence of a chiral edge mode.

Correspondingly, the numerical data under the cylinder geometry indicate the presence of the chiral edge mode [see Fig. 2(a)].

The above results elucidate that the model defined in Eq. (24a) hosts chiral edge modes due to the square-root

topology characterized by the Chern number. Reference 27 has constructed a model whose topology is essentially the same as Eq. (24a). We note however that our approach different from the one used in previous works^{25–27}. While the previous approach^{25–27} is based on the real-space picture, our approach is based on the momentum-space picture, which allows us to construct a model with $N_{\text{Ch},+} = 2$ [see Fig. 2(b)].

C. Three-dimensional system in class CII

Consider a Hamiltonian $H(\mathbf{k})$ for a three-dimensional system of class CII [see Eqs. (1a)-(1c)]. As mentioned in Sec. II A, the squared Hamiltonian $H_{\text{sq}}(\mathbf{k})$ can be block-diagonalized with subsectors of the chiral operator Γ ($\Gamma^2 = 1$).

The squared Hamiltonian $H_{\text{sq},\pm}(\mathbf{k})$ of the plus (minus) sector preserves the time-reversal symmetry with $T^2 = -1$. Therefore, the topology of $H_{\text{sq},\pm}(\mathbf{k})$ can be characterized by the \mathbb{Z}_2 -invariant for three-dimensional systems. As proven in Appendix D topology of the plus sector is the same as topology of the minus sector. In addition, the presence/absence of the additional symmetry does not change the topology (Appendix D).

Therefore, our approach is available for three-dimensional systems in class CII. In the following, we see that a toy model indeed hosts surface states induced by the square-root topology.

1. Surface modes and the topological characterization

Consider the following three-dimensional Hamiltonian,

$$H(\mathbf{k}) = H_{\text{D}}(\mathbf{k}) + m s_1 \tau_1 \rho_0, \quad (26a)$$

$$H_{\text{D}}(\mathbf{k}) = p_1(\mathbf{k}) s_3 \tau_3 \rho_1 + p_2(\mathbf{k}) s_3 \tau_3 \rho_3 + p_3(\mathbf{k}) s_1 \tau_0 \rho_0 + p_4(\mathbf{k}) s_3 \tau_3 \rho_2, \quad (26b)$$

where $\mathbf{k} = (k_x, k_y, k_z)$ denotes the momentum. Prefactors are defined as $p_1(\mathbf{k}) = 2t \sin k_x$, $p_2(\mathbf{k}) = 2t \sin k_y$, $p_3(\mathbf{k}) = 2t \sin k_z$, and $p_4(\mathbf{k}) = 2t(\cos k_x + \cos k_y + \cos k_z) - \mu$. This system preserves the time-reversal and particle-hole symmetry whose operator are defined in Eq. (12).

The squared Hamiltonian $H_{\text{sq}}(\mathbf{k})$ can be block-diagonalized with the matrix $\Gamma = s_3 \tau_1 \rho_0$. The Hamiltonian in the plus sector is written as

$$H_{\text{sq},+}(\mathbf{k}) = [p^2(\mathbf{k}) + m^2] \chi_0 \rho_0 + 2m[p_1(\mathbf{k}) \chi_1 \rho_1 + p_2(\mathbf{k}) \chi_1 \rho_3 + p_3(\mathbf{k}) \chi_3 \rho_0 + p_4(\mathbf{k}) \chi_1 \rho_2]. \quad (27)$$

Here, the plus sector is spanned by a set of the vectors introduced in Sec. II C [see Eqs. (15) and (18)].

As is the case of two-dimensional system [see Sec. II C], the \mathbb{Z}_2 -invariant $\nu_+^{3\text{D}}$ [for the definition see Eq. (D1)] can be computed from the parity eigenvalues of “occupied states” at the time-reversal invariant momenta when the

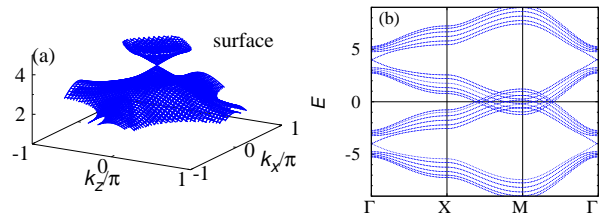


FIG. 3. (a): The surface band structure around $E = 4$. (b): The surface band structure along the high symmetry points, Γ $[(0, 0)]$, X $[(\pi, 0)]$, and M $[(\pi, \pi)]$. These data are obtained for $t = 0.5$, $\mu = 2.3$, $m = 4$. Here, the periodic boundary condition is imposed for the x - and z -direction, while the open boundary condition is imposed for the y -direction. Along the y -direction, $L_y = 6$ sites are aligned.

system is inversion symmetric. We note that $H_{\text{sq},+}(\mathbf{k})$ preserves the inversion symmetry with $P = \chi_1 \rho_2$. Computing the product of the parity eigenvalues at the time-reversal invariant momenta, we can see that the \mathbb{Z}_2 -invariant $\nu_+^{3\text{D}}$ takes one, predicting the presence of surface states.

Correspondingly, Dirac cones can be found around $E \sim \pm 4$ in Figs. 3(a) and 3(b) which are obtained by imposing the periodic (open) boundary condition along the x - and z -directions (the y -direction).

The above results elucidate that the model defined in Eq. (26a) hosts Dirac surface states due to the square-root topology characterized by the \mathbb{Z}_2 -invariant $\nu_+^{3\text{D}}$.

V. CONCLUSION

In this paper, we have analyzed topology of the squared Hamiltonian for systems preserving time-reversal and particle-hole symmetry. Our analysis elucidates that nontrivial topology of the squared Hamiltonian induces helical edge modes at the boundary of the two-dimensional system in class CII in contrast to the absence of the ordinary two-dimensional topological phases in this class.

We have also proposed a method to construct toy models which is complementary to the previous one. Based on our approach, we demonstrate the emergence of helical edge modes in two-dimensional systems of class CII as well as chiral edge modes in two-dimensional systems in class AIII and surface Dirac cones in three-dimensional systems in class CII.

ACKNOWLEDGMENTS

T.Y. thanks Takahiro Fukui for fruitful comments on the \mathbb{Z}_2 -invariant for time-reversal symmetric systems. This work is supported by JPSP Grant-in-Aid for Scientific Research on Innovative Areas “Discrete Geometric Analysis for Materials Design”: Grants No. JP20H04627 (T.Y.). This work is also supported by the JSPS

- ¹ M. Z. Hasan and C. L. Kane, *Rev. Mod. Phys.* **82**, 3045 (2010).
- ² X.-L. Qi and S.-C. Zhang, *Rev. Mod. Phys.* **83**, 1057 (2011).
- ³ K. v. Klitzing, G. Dorda, and M. Pepper, *Phys. Rev. Lett.* **45**, 494 (1980).
- ⁴ D. J. Thouless, M. Kohmoto, M. P. Nightingale, and M. den Nijs, *Phys. Rev. Lett.* **49**, 405 (1982).
- ⁵ B. I. Halperin, *Phys. Rev. B* **25**, 2185 (1982).
- ⁶ Y. Hatsugai, *Phys. Rev. Lett.* **71**, 3697 (1993).
- ⁷ A. Altland and M. R. Zirnbauer, *Phys. Rev. B* **55**, 1142 (1997).
- ⁸ M. R. Zirnbauer, *Journal of Mathematical Physics* **62**, 021101 (2021), <https://doi.org/10.1063/5.0035358>.
- ⁹ C. L. Kane and E. J. Mele, *Phys. Rev. Lett.* **95**, 146802 (2005).
- ¹⁰ C. L. Kane and E. J. Mele, *Phys. Rev. Lett.* **95**, 226801 (2005).
- ¹¹ A. Y. Kitaev, *Physics-Uspekhi* **44**, 131 (2001).
- ¹² W. P. Su, J. R. Schrieffer, and A. J. Heeger, *Phys. Rev. Lett.* **42**, 1698 (1979).
- ¹³ A. P. Schnyder, S. Ryu, A. Furusaki, and A. W. W. Ludwig, *Phys. Rev. B* **78**, 195125 (2008).
- ¹⁴ A. Kitaev, *AIP Conf. Proc.* **1134**, 22 (2009).
- ¹⁵ S. Ryu, A. P. Schnyder, A. Furusaki, and A. W. W. Ludwig, *New J. Phys.* **12**, 065010 (2010).
- ¹⁶ C.-K. Chiu, J. C. Y. Teo, A. P. Schnyder, and S. Ryu, *Rev. Mod. Phys.* **88**, 035005 (2016).
- ¹⁷ K. Hashimoto, X. Wu, and T. Kimura, *Phys. Rev. B* **95**, 165443 (2017).
- ¹⁸ W. A. Benalcazar, B. A. Bernevig, and T. L. Hughes, *Phys. Rev. B* **96**, 245115 (2017).
- ¹⁹ W. A. Benalcazar, B. A. Bernevig, and T. L. Hughes, *Phys. Rev. B* **96**, 245115 (2017).
- ²⁰ F. Schindler, A. M. Cook, M. G. Vergniory, Z. Wang, S. S. P. Parkin, B. A. Bernevig, and T. Neupert, *Phys. Rev. X* **4**, 011012 (2018), [10.1126/sciadv.aat0346](https://doi.org/10.1126/sciadv.aat0346).
- ²¹ E. J. Bergholtz, J. C. Budich, and F. K. Kunst, *Rev. Mod. Phys.* **93**, 015005 (2021).
- ²² T. Yoshida, R. Peters, N. Kawakami, and Y. Hatsugai, *Progress of Theoretical and Experimental Physics* (2020), [10.1093/ptep/ptaa059](https://doi.org/10.1093/ptep/ptaa059), ptaa059.
- ²³ Y. Ashida, Z. Gong, and M. Ueda, *arXiv preprint arXiv:2006.01837* (2020).
- ²⁴ J. Arkininstall, M. H. Teimourpour, L. Feng, R. El-Ganainy, and H. Schomerus, *Phys. Rev. B* **95**, 165109 (2017).
- ²⁵ T. Mizoguchi, Y. Kuno, and Y. Hatsugai, *Phys. Rev. A* **102**, 033527 (2020).
- ²⁶ T. Mizoguchi, T. Yoshida, and Y. Hatsugai, *Phys. Rev. B* **103**, 045136 (2021).
- ²⁷ M. Ezawa, *Phys. Rev. Research* **2**, 033397 (2020).
- ²⁸ J. Attig and S. Trebst, *Phys. Rev. B* **96**, 085145 (2017).
- ²⁹ J. Attig, K. Roychowdhury, M. J. Lawler, and S. Trebst, *Phys. Rev. Research* **1**, 032047 (2019).
- ³⁰ A. Marques, L. Madail, and R. Dias, *arXiv preprint arXiv:2102.12635* (2021).
- ³¹ R. Dias and A. Marques, *arXiv preprint arXiv:2102.00887* (2021).
- ³² Z. Lin, S. Ke, X. Zhu, and X. Li, *Opt. Express* **29**, 8462 (2021).
- ³³ M. Yan, X. Huang, L. Luo, J. Lu, W. Deng, and Z. Liu, *Phys. Rev. B* **102**, 180102 (2020).
- ³⁴ L. Song, H. Yang, Y. Cao, and P. Yan, *Nano Letters* **20**, 7566 (2020), pMID: 32940479.
- ³⁵ This approach is introduced in Ref. 25 and is employed to construct toy models of square-root topological insulators in one and two dimensions in Ref. 27.
- ³⁶ While Ref. 27 has analyzed a one-dimensional system whose squared Hamiltonian becomes Kitaev chain, the physical origin of symmetry of squared Hamiltonian is not clear.
- ³⁷ The absence of the ordinary topological phase can be seen in Table II in Appendix B.
- ³⁸ L. Fu and C. L. Kane, *Phys. Rev. B* **74**, 195312 (2006).
- ³⁹ When the z -component of spins is a conserved quantity, $s = \mathbb{I}$ ($s = \mathbb{II}$) labels the up-spin (down-spin) state.
- ⁴⁰ We consider a Hamiltonian of a $2N \times 2N$ -matrix. The case of $2(N+1) \times 2(N+1)$ -matrix can be discussed by adding a trivial band which does not change the topology.
- ⁴¹ Because $T^2 = -1$ holds, we have $U_T U_T^* = -1$. Recalling that U_T is a unitary matrix, we obtain $U_T = -U_T^\dagger$.
- ⁴² The time-reversal operator for the plus sector is obtained in a similar way as Eq. (16).
- ⁴³ L. Fu and C. L. Kane, *Phys. Rev. B* **76**, 045302 (2007).
- ⁴⁴ We can observe Kramers degeneracy at the time-reversal invariant momenta. The \mathbb{Z}_2 -invariant is obtained⁴³ by computing the product of parity eigenvalues of only “occupied states” labeled with $s = \mathbb{I}$.
- ⁴⁵ For instance, if the topological phases are absent for d -dimensional systems of a given symmetry class preserving the additional symmetry, our approach is not available.
- ⁴⁶ We note that $h_{\text{sq},\pm}(\mathbf{k})$ differs from $H_{\text{sq},\pm}(\mathbf{k})$. The former (latter) is the block-diagonalized Hamiltonian with $U(\Gamma)$.
- ⁴⁷ L. Fu, C. L. Kane, and E. J. Mele, *Phys. Rev. Lett.* **98**, 106803 (2007).
- ⁴⁸ J. E. Moore and L. Balents, *Phys. Rev. B* **75**, 121306 (2007).
- ⁴⁹ R. Roy, *Phys. Rev. B* **79**, 195322 (2009).
- ⁵⁰ T. Fukui and Y. Hatsugai, *Journal of the Physical Society of Japan* **76**, 053702 (2007), <https://doi.org/10.1143/JPSJ.76.053702>.

Appendix A: Proof of Eq. (10)

Firstly, we note the relations $H_{\text{sq},+}(\mathbf{k}) = Q(\mathbf{k})Q^\dagger(\mathbf{k})$ and $H_{\text{sq},-}(\mathbf{k}) = Q^\dagger(\mathbf{k})Q(\mathbf{k})$ which can be seen with the following calculation:

$$H_{\text{sq}} = \begin{pmatrix} Q(\mathbf{k})Q^\dagger(\mathbf{k}) & 0 \\ 0 & Q^\dagger(\mathbf{k})Q(\mathbf{k}) \end{pmatrix}. \quad (\text{A1})$$

The above relations indicate that when $|u_{\pm n}^s(\mathbf{k})\rangle$ are eigenvectors of $H_{\text{sq},+}(\mathbf{k})$, $Q^\dagger(\mathbf{k})|u_{\pm n}^s(\mathbf{k})\rangle$ are eigenvectors of $H_{\text{sq},-}(\mathbf{k})$, which can be seen as follows. For given

eigenstates $|u_{+n}^s(\mathbf{k})\rangle$

$$H_{\text{sq},+}(\mathbf{k})|u_{+n}^s(\mathbf{k})\rangle = |u_{+n}^s(\mathbf{k})\rangle \epsilon_{\text{sq},+sn}(\mathbf{k}), \quad (\text{A2})$$

with eigenvalues $\epsilon_{\text{sq},+sn}(\mathbf{k})$, we have²⁷

$$\begin{aligned} Q^\dagger(\mathbf{k})H_{\text{sq},+}(\mathbf{k})|u_{+n}^s(\mathbf{k})\rangle &= Q^\dagger(\mathbf{k})|u_{+n}^s(\mathbf{k})\rangle \epsilon_{\text{sq},+sn}(\mathbf{k}) \\ \Leftrightarrow H_{\text{sq},-}(\mathbf{k})Q^\dagger(\mathbf{k})|u_{+n}^s(\mathbf{k})\rangle &= Q^\dagger(\mathbf{k})|u_{+n}^s(\mathbf{k})\rangle \epsilon_{\text{sq},+sn}(\mathbf{k}). \end{aligned} \quad (\text{A3})$$

Therefore, $Q(\mathbf{k})|u_{+n}^s(\mathbf{k})\rangle$ are eigenvectors of $H_{\text{sq},-}(\mathbf{k})$.

Assuming that eigenvalues of $H(\mathbf{k})$ are non-zero [i.e., $\epsilon_{\text{sq},+sn}(\mathbf{k})$ are positive], the normalized eigenvectors are written as

$$|u_{-n}^s(\mathbf{k})\rangle = \frac{1}{\sqrt{\epsilon_{\text{sq},+sn}(\mathbf{k})}} Q^\dagger(\mathbf{k})|u_{+n}^s(\mathbf{k})\rangle, \quad (\text{A4})$$

with the normalized eigenvectors $|u_{+n}^s(\mathbf{k})\rangle$.

In addition, $|u_{-n}^s(\mathbf{k})\rangle$ satisfy the time-reversal constraint [Eq. (6)], provided that $|u_{+n}^s(\mathbf{k})\rangle$ satisfy it. This can be seen by noting the relation

$$U_T Q^*(\mathbf{k}) U_T^\dagger = Q(-\mathbf{k}), \quad (\text{A5})$$

which holds because $H(\mathbf{k})$ preserves the time-reversal symmetry [see Eqs. (1a) and (9)]. Namely, applying T , we have

$$\begin{aligned} T|u_{-n}^s(\mathbf{k})\rangle &= \frac{1}{\sqrt{\epsilon_{\text{sq},+sn}(\mathbf{k})}} U_T Q^T(\mathbf{k}) \mathcal{K} |u_{+n}^s(\mathbf{k})\rangle \\ &= \frac{1}{\sqrt{\epsilon_{\text{sq},+sn}(\mathbf{k})}} Q^\dagger(-\mathbf{k}) U_T \mathcal{K} |u_{+n}^s(\mathbf{k})\rangle \\ &= \frac{1}{\sqrt{\epsilon_{\text{sq},+sn}(\mathbf{k})}} Q^\dagger(-\mathbf{k}) T |u_{+n}^s(\mathbf{k})\rangle \\ &= \text{sgn}(s) \frac{1}{\sqrt{\epsilon_{\text{sq},+sn}(\mathbf{k})}} Q^\dagger(-\mathbf{k}) |u_{+n}^{\bar{s}}(-\mathbf{k})\rangle, \\ &= \text{sgn}(s) \frac{1}{\sqrt{\epsilon_{\text{sq},+\bar{s}n}(-\mathbf{k})}} Q^\dagger(-\mathbf{k}) |u_{+n}^{\bar{s}}(-\mathbf{k})\rangle, \end{aligned} \quad (\text{A6})$$

where \bar{s} takes I (II) for $s = \text{II}$ (I). The function $\text{sgn}(s)$ takes 1 (−1) for $s = \text{I}$ (II). From the first and the second line we have used Eq. (A5). We note that for time-reversal symmetric $H_{\text{sq},+}(\mathbf{k})$, the relation $\epsilon_{\text{sq},+\bar{s}n}(-\mathbf{k}) = \epsilon_{\text{sq},+sn}(\mathbf{k})$ holds.

The above results prove Eq. (10).

Appendix B: Derivation of Table I

The classification results for systems with the additional symmetry [see Eq. (19)] can be obtained by analyzing the symmetry constraints imposed on the block-diagonalized Hamiltonian⁴⁶ $h_{\text{sq},\pm}(\mathbf{k})$ with U ($U^2 = 1$).

class A, class AI, and class AII, −. In the absence of particle-hole and chiral symmetry, we can take the identity matrix as U satisfying Eq. (19). Thus, the classification results are identical to the ordinary ones.

class	T	C	Γ	$d = 0$	$d = 1$	$d = 2$	$d = 3$
\S A	0	0	0	\mathbb{Z}	0	\mathbb{Z}	0
AIII	0	0	1	0	\mathbb{Z}	0	\mathbb{Z}
$\S\S$ AI	1	0	0	\mathbb{Z}	0	0	0
BDI	1	1	1	\mathbb{Z}_2	\mathbb{Z}	0	0
D	0	1	0	\mathbb{Z}_2	\mathbb{Z}_2	\mathbb{Z}	0
DIII	-1	1	1	0	\mathbb{Z}_2	\mathbb{Z}_2	\mathbb{Z}
$\S\S\S$ AII	-1	0	0	\mathbb{Z}	0	\mathbb{Z}_2	\mathbb{Z}_2
CII	-1	-1	1	0	\mathbb{Z}	0	\mathbb{Z}_2
C	0	-1	0	0	0	\mathbb{Z}	0
CI	1	-1	1	0	0	0	\mathbb{Z}_2

TABLE II. Classification results of ordinary topological insulators and superconductors^{13–15}. From the first and the fourth column specify the symmetry of systems. The second (third) column describes the presence/absence of the time-reversal (particle-hole) symmetry; for instance, in the second column, “±1” indicates presence of time-reversal symmetry [Eq. (1a)] described by the time-reversal operator $T^2 = \pm 1$ while “0” indicates the absence of the symmetry. In the fourth column, “1” (“0”) indicates the presence (absence) of the chiral symmetry [Eq. (1c)].

class AIII−. Equation (19c) indicates that the chiral symmetry is not closed for the subsectors; no symmetry constraint is imposed on $h_{\text{sq},+}(\mathbf{k})$. Thus, $h_{\text{sq},+}(\mathbf{k})$ belongs to class A. Therefore, the classification result is obtained from the row marked with “ \S ” in Table II.

class BDI and class CI−. Equation (19) indicates that only time-reversal symmetry ($T^2 = 1$) is closed for each subsector; particle-hole symmetry and chiral symmetry are not closed. Thus, $h_{\text{sq},+}(\mathbf{k})$ belongs to class AI. Here, we note that the result is not affected by whether C^2 is equals to 1 or −1. Therefore, the classification result is obtained from the row marked with “ $\S\S$ ” in Table II.

class DIII and class CII−. Equation (19) indicates that only time-reversal symmetry ($T^2 = -1$) is closed for each subsector; particle-hole symmetry and chiral symmetry are not closed. Thus, $h_{\text{sq},+}(\mathbf{k})$ belongs to class AII. As is the previous case, the result is not affected by whether C^2 is equals to 1 or −1. Therefore, the classification result is obtained from the row marked with “ $\S\S\S$ ” in Table II.

class D and class C−. Equation (19b) indicates that the particle-hole symmetry is not closed for the subsectors; no symmetry constraint is imposed on $h_{\text{sq},+}(\mathbf{k})$. Thus, $h_{\text{sq},+}(\mathbf{k})$ belongs to class A. As is the previous case, the result is not affected by whether C^2 is equals to 1 or −1. Therefore, the classification result is obtained from the row marked with “ \S ” in Table II.

Appendix C: Topology of the squared Hamiltonian of class AIII in two dimensions

The squared Hamiltonian $H_{\text{sq}}(\mathbf{k})$ can be block-diagonalized with Γ ($\Gamma^2 = 1$). In this appendix, we show

the following facts. (i) The topology of the plus sector is same as the topology of the minus sector. (ii) The presence/absence of the additional symmetry does not affect the topology.

Firstly, we show that the topology of the plus sector is same as the topology of the minus sector [see Eq. (C2)] Because the chiral symmetry is not closed for each subsector, the block-diagonalized Hamiltonian $H_{\text{sq},\pm}$ is characterized by the Chern number

$$N_{\text{Ch},\pm} = \int \frac{dk_x dk_y}{2\pi i} F_{\pm}(\mathbf{k}), \quad (\text{C1a})$$

with

$$A_{\pm,\mu}(\mathbf{k}) = \langle u_{\pm n}(\mathbf{k}) | \partial_{\mu} | u_{\pm n}(\mathbf{k}) \rangle, \quad (\text{C1b})$$

$$F_{\pm}(\mathbf{k}) = \partial_x A_{\pm,y} - \partial_y A_{\pm,x}. \quad (\text{C1c})$$

Here, $|u_{\pm n}(\mathbf{k})\rangle$ denote eigenvectors of $H_{\text{sq},\pm}$ with eigenvalues $\epsilon_{\text{sq},\pm n}(\mathbf{k})$.

Now, we show that the relation

$$N_{\text{Ch},+} = N_{\text{Ch},-}, \quad (\text{C2})$$

holds.

Consider the case where the eigenvalues are non-zero and the Hamiltonian $H(\mathbf{k})$ is written as

$$H(\mathbf{k}) = \begin{pmatrix} 0 & Q(\mathbf{k}) \\ Q^{\dagger}(\mathbf{k}) & 0 \end{pmatrix}, \quad (\text{C3})$$

with $N \times N$ -matrix $Q(\mathbf{k})$ which maps a state in the minus sector of Γ to a state in the plus sector.

As is the case of Eq. (10), we can see that $|u_{-n}(\mathbf{k})\rangle$ is obtained from $|u_{+n}(\mathbf{k})\rangle$,

$$|u_{-n}(\mathbf{k})\rangle = \frac{1}{\sqrt{\epsilon_{\text{sq},+n}(\mathbf{k})}} Q^{\dagger}(\mathbf{k}) |u_{+n}(\mathbf{k})\rangle, \quad (\text{C4})$$

with the eigenvalues of the squared Hamiltonian for the plus sector $\epsilon_{\text{sq},+n}(\mathbf{k})$.

Thus, we have

$$A_{-, \mu}(\mathbf{k}) = A_{+, \mu}(\mathbf{k}) + f_{\mu}(\mathbf{k}) \quad (\text{C5a})$$

with

$$f_{\mu}(\mathbf{k}) = \frac{1}{\sqrt{\epsilon_{\text{sq},+n}(\mathbf{k})}} \text{tr} \left[P_{+}(\mathbf{k}) Q(\mathbf{k}) \left(\partial_{\mu} \frac{1}{\sqrt{\epsilon_{\text{sq},+n}(\mathbf{k})}} Q^{\dagger}(\mathbf{k}) \right) \right], \quad (\text{C5b})$$

$$P_{+}(\mathbf{k}) = \sum_n |u_{+n}\rangle \langle u_{+n}|. \quad (\text{C5c})$$

Applying Stokes' theorem to Eq. (C1), we can see that the integral of $f_{\mu}(\mathbf{k})$ vanishes because $f_{\mu}(\mathbf{k})$ is gauge independent. The above results prove Eq. (C2).

Now, we show that the presence of the additional symmetry U does not change the topology. For systems with the additional symmetry, applying U just maps a state in the plus sector of Γ to a state in the minus sector. This fact results in Eq. (C2) which is satisfied even without the additional symmetry.

Appendix D: Topology of the squared Hamiltonian of class CII in three dimensions

The squared Hamiltonian $H_{\text{sq}}(\mathbf{k})$ can be block-diagonalized with Γ ($\Gamma^2 = 1$). In this appendix, we show the following facts. (i) The topology of the plus sector is same as the topology of the minus sector. (ii) The presence/absence of the additional symmetry does not affect the topology.

Firstly, we show that the topology of the plus sector is same as the topology of the minus sector. Because only time-reversal symmetry is closed for the block-diagonalized subsector, the topology of $H_{\text{sq},\pm}(\mathbf{k})$ is characterized by the \mathbb{Z}_2 -invariant⁴⁷⁻⁴⁹ for three-dimensional systems $\nu_{\pm}^{3\text{D}}$. For systems whose BZ is cubic, $\nu_{\pm}^{3\text{D}}$ is defined as^{47,48,50}

$$\nu_{\pm}^{3\text{D}} = \nu_{\pm}(0)\nu_{\pm}(\pi). \quad (\text{D1})$$

Here, $\nu_{\pm}(k_z^*)$ ($k_z^* = 0, \pi$) are \mathbb{Z}_2 -invariants computed for two-dimensional BZs specified by k_z^* . Specifically, $\nu_{\pm}(k_z^*)$ is given by

$$\nu_{\pm}(k_z^*) = \frac{1}{2\pi i} \left[\int_{-\pi}^{\pi} dk_x [A_{\pm,x}(k_x, \pi, k_z^*) - A_{\pm,x}(k_x, 0, k_z^*)] - \int_{-\pi}^{\pi} dk_x \int_{-\pi}^0 dk_y F_{\pm}(\mathbf{k}) \right]. \quad (\text{D2})$$

The Berry connection $A_{\pm,\mu}$ ($\mu = x, y$) and the Berry curvature $F(\mathbf{k})$ are defined in Eq. (5a). For commutation of $\nu_{\pm}(k_z^*)$, the gauge is chosen so that Eq. (6) is satisfied.

Here, we show that

$$\nu_{+}^{3\text{D}} = \nu_{-}^{3\text{D}}, \quad (\text{D3})$$

holds, which can be proven in a similar way to the case of two dimensions (see Sec. II B 2 and Appendix A). As is the case of the two-dimensional systems we have

$$\nu_{+}(k_z^*) = \nu_{-}(k_z^*), \quad (\text{D4})$$

without requiring the additional symmetry. Because the $\nu_{\pm}^{3\text{D}}$ is computed from $\nu_{\pm}(k_z^*)$ [see Eq. (D1)], we can see that Eq. (D3) holds.

Now, we show that the additional symmetry U does not affect the topology. For systems with the additional symmetry, applying U just maps a state in the plus sector of Γ to a state in the minus sector [see Eq. (19c)]. This fact results in Eq. (D3) which holds even without the additional symmetry.